Accepted Manuscript

Energy saving potential of a counter-flow regenerative evaporative cooler for various climates of China: Experiment-based evaluation

Zhiyin Duan[a*], Xudong Zhao[b], Changhong Zhan[c], Xuelin Dong[d], Hongbing Chen[a]

[a] Beijing Key Lab of Heating, Gas Supply, Ventilating and Air Conditioning Engineering, Beijing University of Civil Engineering and Architecture, Beijing 100044, China

[b] University of Hull, Hull, HU6 7RX, UK

[c] School of Architecture, Heilongjiang Cold Climate Architectural Science Key Laboratory, Harbin Institute of Technology, 66 Xidazhi Street, Harbin 150001, China

[d] Key Laboratory of Petroleum Engineering, China University of Petroleum, Beijing 102249, China

[*]Corresponding author. Tel:+86 10 68322535

E-mail address: duanzhiyin@bucea.edu.cn (Z. Duan)

Highlights:

- Development a type of evaporative medium with high wickability performance
- Design and construction of a high performance counter-flow REC/HMX
- Experimental results of the REC system in various test conditions of China
- Providing an experiment-based method for estimating REC's energy saving potentials
- Power demands saved by the REC for China's various climates were found

Abstract:

Recently there has been growing interest in regenerative evaporative coolers (REC), which can reduce the temperature of the supply air to below the wet-bulb of intake air and approach its dew-point. In this paper, we designed, fabricated and experimentally tested a counter-flow REC in laboratory. The REC's core heat and mass exchanger was fabricated using stacked sheets composed of high wicking evaporation (wickability of available materials was measured) and waterproof aluminium materials. The developed REC system has a much higher cooling performance compared to conventional indirect evaporative cooler. However, the decision to use the REC for China buildings depends on a dedicated evaluation of the net energy saved against the capital expended. Such an evaluation requires the hourly-based data on the availability of cooling capacity provided by the REC for various climates. The paper used an experiment-based method to estimate the cooling capacity and energy savings provided by the proposed REC for China's various climates. By using the experimental results and regional hourly-based weather data, the energy saving potential of the REC against an equivalent-sized mechanical air conditioner alone was analysed. The results indicate that, for all selected regions, the REC could reduce 53-100% of cooling load and 13-58% of electrical energy consumption annually.

Nomenclature

C_p	specific heat of outlet air, kJ/kg K
E	energy change in airstream, kW
h	enthalpy of moist air, kJ/kg
m	mass flow rate, kg/s
P	electrical power consumptions, kW
Q	cooling capacity, kW
Q_{in}	internal cooling load of building, kW
Q_c	total cooling capacity required to satisfy indoor design condition, $Q_c = Q_{in}$, kW
t	temperature, ºC

V	volume flow rate, m³/h

Greek letters

ε	cooling effectiveness
ρ	density of air, kg/m³

Subscripts

1	inlet air of product channels
2	outlet air of product channels
3	exhaust air of working channels
cond	condensing unit in PUA
db	dry-bulb
fan	fan for circulating primary air through the cooling coil of PUA
hybrid	hybrid cooling system integrated REC and PUA
in	indoor design condition
out	outdoor design condition
p	product air
PUA,S	stand-alone PUA
w	working air
wb	wet-bulb

Abbreviations

CDBT	coincident dry-bulb temperature, ℃
COP	coefficient of performance
CSWD	Chinese Standard Weather Data
CWBT	coincident wet-bulb temperature, ℃
DBT	dry-bulb temperature, ℃
HMX	heat and mass exchanger

IEC   indirect evaporative cooler

PREC   percentage of cooling capacity provided by the REC unit, %

PUA   package unit air conditioner

RH   relative humidity, %

REC   regenerative evaporative cooler

SEC   saving of energy consumption, %

SSEC   seasonal saving of electricity consumption, %

Std P   standard pressure, kPa

WBD   wet-bulb depressions, i.e. temperature difference between db and wb,
               ^{o}C

WBT   wet-bulb temperature, ^{o}C

Keywords: Evaporative cooling; Regenerative evaporative cooler; Experimental test; Evaporative material; Wickability measurements

1 Introduction

Vapour compression refrigeration systems, as the most popular air conditioning system in the world, consume large amounts of electrical energy due to the participation of compressors. Indirect evaporative coolers (IEC), using the latent heat of water vaporisation to remove the heat from airflow without adding moisture, have a great potential of providing sensible cooling for buildings at the cost of low energy consumption. However, the IEC is limited by wet-bulb temperature (WBT) of inlet air that impede its wide application, especially when applied in hot and humid outdoor conditions where the wet-bulb temperature is high, the IEC system may provide inadequate cooling capacity for buildings.

Over the last decades, many efforts have been made to combine typical IEC system with direct evaporative cooler [1], liquid cooled water chiller system or vapour compression air conditioners [2–5] in order to enhance system's overall efficiency and obtain significant energy-saving effect. Quite a few works have been concentrated on integrating liquid desiccant system prior to the IEC system in order to reduce the humidity of air entering the IEC [6–9]. The hybrid dehumidification and IEC systems could produce about 10-80% energy savings [7,10]. The energy saving potentials of those hybrid systems, applied in dry, moderately humid,

4

hot and humid climates, have been extensively evaluated based on the methodologies including theoretical analysis [2,11], detailed energy simulation [4,7,10,12] and field/laboratory experiment data [3,5,11]. There have been found that the hybrid IEC and vapour compression cooling system could provide great amount of energy savings for hot and dry climate, such as nearly 75% of cooling load and 55% energy reductions for Iran [3], 15% and 10-70% energy savings for Delhi [12] and Saudi Arabia [5] respectively. For hot and humid climate, about 35-47% of cooling load could be removed by the hybrid IEC system [4]. Despite of considerable energy-saving potentials, as opposed to stand-alone IEC, these hybrid systems are still more complex in the aspects of system configurations as well as operating modes and are more expensive for capital cost.

More recently there has been growing interest in regenerative evaporative cooler (REC), which alone has the ability to produce supply air temperature below the wet bulb of intake air and approaching the dew point [13–15]. Fig. 1 demonstrates the basic working principles of two types of REC heat and mass exchanger (HMX), i.e. Maisotsenko-cycle (M-cycle) and single-stage regenerative HMX and their related psychrometric thermal processes. For M-cycle regenerative HMX, as shown in Fig. 1(a), part of the dry surface is designed for the product air to pass through while the rest is allocated to the working air. Both the product and working air flow parallel along the dry channels. There are numerous perforations evenly distributed over the surface where the working air is contained and each of these allows a portion of air to enter into the wet channel. Through the small holes, all of the air in working dry channel is gradually diverted to the wet surface as it flows along the dry side. This part of dry air, as working air, is pre-cooled before entering the wet side by losing heat to the adjacent wet surface. The working air flowing over the wet surface of wet channels absorbs heat from the product and working air of dry sides. During this process (see psychrometric chart of Fig. 1(a)), the temperature of product air is reduced at constant humidity ratio, while the working air is partially pre-cooled, humidified and heated in multi-stage process (1-2'-2'wb-3', 2'-2"-2"wb-3", 2"-2'''-2'''wb-3''', 2'''-2-2wb-3) before it is exhausted to the outside. The working air in this cooler is capable of absorbing more heat from the adjacent product and working dry sides, resulting in higher cooling effectiveness against typical indirect evaporative cooler.

In comparison to the M-cycle flow arrangement, Fig. 1(b) shows a type of REC HMX with even higher cooling effectiveness (but with higher pressure loss) [16]. This type of exchanger works as follows: The product air enters into the exchanger from the inlet of dry channel and flows along the channels. Through the penetrations at the end of channel, a certain percentage of the product air, as all of the working air, is redirected into the adjacent wet channel. In this thermal process, as represented in the psychrometric chart of Fig. 1(b), product air is cooled along the dry channels without any increase in humidity, while the working air is initially cooled to the minimum with rise in humidity at a certain distance from the entrance due to the effects of water evaporation. After that, the working air temperature begins to go up in the remainder of the wet channel because the sensible heat transfer from product air in dry sides exceeds the effect of evaporation cooling [17]. This unique arrangement allows the working air to be fully cooled before entering the working channel, thus leading to increased temperature difference and heat transfer between working and product air.

In recent years, many studies have been conducted to develop simplified or complicated numerical models for the regenerative HMX based on M-cycle cross-flow and counter-flow configurations [16,19–25]. The achieved results have been used for 1) predicting/comparing

5

their different performance and characteristics as well as 2) evaluating the effects of geometrical and operating parameters on HMX's performance and 3) optimising flow patterns and structures of HMX. A few laboratory and on-site experimental works [24,26–31] have also been carried out to obtain operating performance of the cross-flow and counter-flow HMX under various inlet conditions, which were used for verifications of the theoretical results obtained from numerical modelling.

The cross-flow configuration based on M-cycle conception has been commercialised in the USA by Idalex Inc. and Coolerado Corp. [32]. However the single-stage counter-flow regenerative HMX is still at research and development stage. In this paper, we designed, fabricated and experimentally tested a single-stage counter-flow HMX/REC system under various climates of China. The developed REC system has a much higher cooling performance compared to conventional IEC. However, the decision to apply the proposed regenerative HMX/REC system for China's buildings depends largely on an in-depth assessment of net energy saved against capital cost. Such an assessment requires hourly data on the availability of cooling capacity provided by the REC for locations with various climates, particularly for regions with hot and humid climate, in which the REC's incapable of providing full cooling demands. This paper quantifies in-depth cooling availability and energy-savings provided by the newly-developed counter-flow REC system for a wide range of regions in China, including Beijing, Shanghai, Guangzhou, Chongqing, Lanzhou, Xi'an, Harbin and Urumqi, and suggests a method of assessing such data for any world wide location where meteorological records are available. The paper incorporates the experimental findings and bases the analysis of cooling availability and energy-saving potential on meteorological test reference weather year data. This work confirms the technical and economic viability of the technique to be used in various locations of China through the dedicated experiments and extensive evaluation of cooling and energy saving potential to be undertaken.

2 Descriptions and design considerations of the proposed REC and HMX

2.1 Counter-flow regenerative HMX

As demonstrated in Fig. 2(a), a self-contained counter-flow REC was designed and fabricated in this study. The cooler mainly includes a counter-flow regenerative HMX, a supply air fan, an exhaust air fan, a water distributor, a water reservoir, a water pump, louvers and an enclosure. In this exchanger, product air, entering the dry channel from bottom, is cooled along the path and discharged on the top. Through the perforations at the end, a portion of product air, as working air, is extracted and diverted into the adjacent wet channel. The working air flows downwards in the counter direction to the product air in the dry channel and finally discards to the outside.

As depicted in Fig. 2(b), the dry and wet channel was composed of water-repellent aluminium surface and water-retaining wicking surface respectively. The dry and wet channels are equally 900 mm in length, 6 mm in height and 314 mm in width. Thickness of the heat transfer plate between dry and wet channel is 0.25 mm. The corrugated sheets used as air guiders for the dry and wet channels are equally 900 mm in length, 314 mm in width and 5.8 mm in height. Pitches of the corrugated sheet in dry and wet channels are equally 12 mm.

For the HMX, the reasons to choose the counter-flow configuration are motivated by following considerations: 1) the noticeable advantages of counter-flow configuration include

high cooling effectiveness and ease of construction. Although, its disadvantage is less energy efficiency than the cross-flow configuration considering the equivalent geometric size and inlet conditions [16]; 2) for the cross-flow configuration with larger ratio of dry channel length to wet channel length, the deteriorating effect of longitudinal heat condition on the effectiveness of cross-flow configuration is higher than that of counter-flow configuration [33]. Therefore, a counter-flow configuration was employed and a slim structure was designed to reduce the effect of longitudinal heat conduction in the exchanger walls of a compact-plate counter-flow indirect evaporative cooler [34].

2.2 Material of HMX

The decision to choose suitable material for constructing the HMX is based on overall consideration of low capital cost and high performance. In this study, the construction of the plate heat exchanger utilises a type of cellulose-blended fibre with the features of high water retention and wickability as the wet channel, while the dry channel uses a moisture-impervious aluminium film to maintain high strength and machinability. The wicking surface of fibre was coated onto the surface of moisture-impervious film by using reactive hydrophilic adhesive. The wicking performance was significantly improved as a result of this treatment.

2.3 Wickability measurements of evaporative medium

The height approach: The vertical wicking height of available hydrophilic materials was measured and compared to attain the ideal evaporative surface used in fabricating heat exchanger. A schematic of test apparatus (measurement range: 0-200 mm, 1mm resolution) and the experimental setup is shown in Figs. 3(a) and 3(b) respectively. In the test, as shown in Fig. 3(a), samples of test surface are hung on a holder at the top, while the bottom edges are vertically dipped in a water reservoir (water was dyed to mark the water level). The height that the water travels in a certain length of time is measured. Several types of samples, as shown in Table 1, were dipped vertically 1.3 mm below the water level of reservoir. The water immediately wicked upwards through the test surface.

This wicking process was being continuously recorded for 2 hours until wicking height reach equilibrium. This is the wicking height where capillary forces on the water are balanced by the weight of the water. Fig. 4 shows the wicking height as a function of time for the different test samples. Water level of reservoir was used as the datum line for measuring the wicking height, and the height was measured along the middle axis of the surface. It was found that the wicking height of "material H" was dramatically growing within 5-miniute reaching 90% of maximum wicking height that was finally achieved after 2 hours. Its remarkable capability of fast wetting enables the evaporative cooler to generate adequate cooling immediately after being started. In contrast, "material I" was less wickable than "material H" within 50 minutes approximately, but its wicking height exceeded that of "material H" and still continuously increasing afterwards.

The mass approach: Wickability was also measured by mass approach to see if the surface thickness had an effect on the wicking performance.

In this approach, the test samples were prepared to have equal surface area and dipped into a water sink as in the height approach for the same period of time until they were saturated. The test samples were then removed and weighted immediately in a Kern PCB 250-3 precision

scale (measurement range:0-250 g, 0.001 g resolution). The weight of water wicked was accomplished by subtracting the dry weight form the wet weight. Fig. 5 plots the weight of water wicked per unit thickness for the available samples. The wicked mass was divided by thickness to eliminate the effect of difference in material thickness. Among the test samples, "material H" had the highest mass of wicked water whereas "material E" had the lowest value.

The measurements of wicking height and mass taken above show that the "material H", i.e. cellulose-blended fibre coated aluminium sheet has the highest wickability among others. This type of material was finally used to fabricate the heat exchanger of REC for the purpose of achieving complete wetting and high water retention.

3. Performance indicators for REC

The extent to which the outlet air temperature delivered by the cooler approaches the wet-bulb temperature of the inlet air is expressed as wet-bulb effectiveness ε_{wb}, which is determined as:

$$\varepsilon_{wb} = \frac{t_{db,1} - t_{db,2}}{t_{db,1} - t_{wb,1}} = \frac{t_{db,1} - t_{db,2}}{WBD} \tag{1}$$

Cooling capacity of the REC is defined as:

$$Q_{REC} = \frac{V_2 \rho C_p (t_{db,1} - t_{db,2})}{3600} = \frac{V_2 \rho C_p \varepsilon_{wb} WBD}{3600} \tag{2}$$

Coefficient of performance of the REC is defined as the cooling capacity divided by total electrical power consumption of fans and water pump in the REC, which is given bellow:

$$COP_{REC} = \frac{Q_{REC}}{P_{REC}} \tag{3}$$

4. Experimental setup of REC system and testing procedure

4.1 Experimental setup

Sets of dedicated experiments were conducted to investigate performance characteristics of the presented REC system under typical climatic conditions of China. The experimental data were collected to provide adequate information for predicting system performance, and therefore to evaluate the annual energy consumptions for various climates. Through the experimental results and detailed analysis, the annual energy savings achieved by the REC for different locations were calculated in order to evaluate its regional technical viability.

A schematic of the experimental setup is shown in Fig 6. The experiment system includes the stand-alone REC unit, an inlet air pre-treatment unit and a supply air duct. The inlet air pre-treatment unit consists of an electric heater, a humidifier, an intake air fan and a filter, which was used to adjust the air temperature, humidity and velocity entering the REC unit. The velocities of supply and exhaust air were adjusted by supply and extraction fan respectively. By adjusting the speeds of supply and extraction fans simultaneously, the ratio of exhaust to intake airflow rate, namely working-to-intake air ratio, was set to achieve higher supply airflow

8

rate and cooling effectiveness. The speeds of intake, supply and extraction fans were fixed at certain settings to obtain low temperature of supply air. To measure the average dry-bulb temperature of intake, supply and exhaust air, numerous K-type thermocouples (±1.5 K error after calibration) were located at various positions on the cross section of connecting circular ducts to obtain weighted mass flow average of the measured data. Fig. 7 shows a view of the experimental setup.

Velocities of the intake, supply and exhaust air were measured by Testo 425 hotwire anemometers (±0.03 m/s error). The mean velocity for each airflow was determined by taking arithmetic average of the numerous measured points. Relative humidity of intake, supply and exhaust airflows were measured using calibrated Visalia HMP45A humidity probe ($\pm1\%$ RH error after calibration), which was fitted to the centre of the measured cross section. The electrical power was measured by a 3PH Watt Meter (±0.1 W error). Those measured data of thermocouples and humidity probes were recorded and transferred to a computer through a data logger (DT500 Datataker). An internal programme was compiled in the logger for data acquisition and analysis. The measured data were analysed under steady states which was defined as the period when variations of temperature and humidity are within 0.1 ºC and 1% RH for continuous 15 minutes. Once steady state had been reached, the temperature and humidity used to perform the analysis were determined by taking the average of numerous measured data over 10-minute intervals. The data collected enabled a number of performance indicators to be determined including wet-bulb effectiveness, supply airflow rate, cooling capacity, power consumption and COP.

4.2 Uncertainty analysis of experimental results

The measurement accuracy of experiment is affected by the locations of testing sensors. Particularly, the accuracy of airflow rate evaluated from the air velocity measurement depends largely on uniformity of the air velocity distribution. Energy changes between the product and working air of dry and wet channels were calculated by Eqs. (4) and (5) respectively to verify the accuracy of airflow rate and measuring positions of sensors. Fig. 8 illustrates the comparison of energy changes in dry channel and wet channel for all experimental results. It is shown that the energy changes between them agree well and the inconsistency is less than 5%.

$$E_p = m_1 \left(h_1 - h_2 \right) \tag{4}$$

$$E_w = m_3 \left(h_3 - h_2 \right) \tag{5}$$

Eq. (6) can be used to determine the relative uncertainty for the dependent performance indicator variables.

$$\frac{\Delta y}{y} = \sqrt{\sum_i \left(\frac{\partial y}{\partial x_i} \cdot \frac{\Delta x_i}{y} \right)^2} \tag{6}$$

Where $\Delta y/y$ represents the relative uncertainty of dependent variables, i.e. $\Delta\varepsilon_{wb}/\varepsilon_{wb}$, $\Delta Q_{REC}/Q_{REC}$, $\Delta COP_{REC}/COP_{REC}$; y is the function of independent variables x_i described in the Eqs. (1)-(3) respectively. For instance, $y=\varepsilon_{wb}$, thus $x_i=t_{db,1}$, $t_{db,2}$, $t_{wb,1}$. The uncertainty for the

performance indicator variables was found to be within ±2.0% for wet-bulb effectiveness, ±5.3% for sensible cooling capacity and ±5.3% for COP on average.

4.3 Test conditions

Test conditions were selected to evaluate performance of the REC system over a range of ambient conditions that adequately represent typical climatic conditions found during the cooling season (June-September) at various regions of China. Due to the vast land area and highly diverse topography, the climate zones in China are categorised into 5 distinct zones including "severe cold", "cold", "mild", "hot summer and cold winter" as well as "hot summer and warm winter" zones. From these typical zones, 15 representative cities were selected and the summer climatic design conditions for these cities obtaining from ASHRAE Handbook of Fundamentals [35] are presented in Table 2. The design conditions include cooling and evaporation design conditions that are exceeded less than 0.4% of a year on average. The cooling design conditions, including DBT and coincident wet-bulb temperature (CWBT), are used in calculating cooling load of buildings; Evaporation conditions, including WBT and coincident dry-bulb temperatures (CDBT) are used in sizing cooling tower and other evaporation equipment. These conditions were plotted on a psychometric chart (Fig. 9) to determine test points that cover the majority of design conditions for the selected regions. These test points (marked with 38 indices), representing the possible intake air conditions of the REC, are indicated on Fig. 10. According to the test conditions, the intake air conditions of experimental set-up were set to acquire the REC's performance data. By using the experiment data, hourly Chinese Standard Weather Data (CSWD) [36] and the analytical approach described in the next section, the system's performance and associated energy saving potential for different regions were calculated. ASHRAE summer thermal comfort zone is also highlighted in Fig. 10 to indicate the scope of conditions that should be maintained to keep most occupants in a space comfortable. The air supplied to the space should be at a condition to the left and slightly below the summer comfort zone to allow for sensible and latent heat gains within the space. For some cases, 100% fresh air could be used directly to provide cooling for a space when outdoor air temperature is low enough. For instance, the south-western regions of China have "mild" outdoor design DBT, such as Xining, Lhasa or Kunming (zone 4) where the natural outdoor air is adequate for cooling requirements of building for the most of summer time. However, for buildings in other regions, there would have great possibilities of requiring air conditioning during summer.

*Note: Climate zone from 1 to 5 represents "severe cold", "cold", "mild", "hot summer and cold winter" as well as "hot summer and warm winter" respectively.

5 Analytical methodology of annual energy saving potential

We used an example building to determine annual/seasonal energy saving potential of REC as pre-cooler in various climates of China. The building is served by the REC unit and a conventional packaged unit air conditioner (PUA). Assuming the building fresh air requirement is 127 m³/h. The summer indoor design condition is 24 ºC dry-bulb and 50% RH, which gives an enthalpy of 48.33 kJ/kg. The outdoor design conditions of selected regions are specified in Table 2. The building internal cooling load is determined by the given equation:

$$Q_{in} = \frac{V_{out}\rho(h_{out} - h_{in})}{3600} \tag{7}$$

The REC unit is used to bring the outdoor air condition approach to the room air condition for the purpose of reducing the impact of cooling load on the PUA. The cooling capacity of REC, Q_{REC}, is determined by Eq. (2).

Provided that the internal cooling load cannot be covered by the REC completely, conventional PUA should be used to fulfil the remaining load. To determine the cooling capacity delivered by the PUA, Q_{PUA}, the following equation is given:

$$Q_{PUA} = Q_c - Q_{REC} = Q_{in} - Q_{REC} \tag{8}$$

Percentage of cooling capacity provided by the REC unit, i.e. PREC, can be estimated as below:

$$PREC = \frac{Q_{REC}}{Q_{REC} + Q_{PUA}} \times 100\% \tag{9}$$

Power consumptions of the hybrid REC and PUA system are calculated as follows:

$$P_{hybrid} = P_{REC} + P_{PUA} \tag{10}$$

$$P_{PUA} = \frac{Q_{PUA}}{COP_{cond}} + P_{fan} \tag{11}$$

The compressor, condenser fans and the air distribution fan are the important power consumers of a PUA. The COP of the condensing unit, representing the combined power of the compressor and the condenser fans of a packaged unit as a function of ambient dry-bulb temperature, can be obtained by the following empirical formula [37]:

$$COP_{cond} = 4.801 - 0.0612 t_{db,1} \tag{12}$$

Where, P_{fan}=additional fan power for circulating 127 m^3/h of the primary air through the cooling coil of the PUA and filter is 12.6 W, assuming a pressure drop of 200 Pa. The energy efficiency of fan and motor is 70% and 80% respectively.

Saving of energy consumption of the hybrid REC and PUA system is accomplished by:

$$SEC = \left(1 - \frac{P_{hybrid}}{P_{PUA,S}}\right) \times 100\% \tag{13}$$

where, $P_{PUA,S}$ determined by Eq. (11), is the power consumed by a stand-alone PUA used for delivering the equal cooling capacity with Q_c.

To evaluate energy saving potential of the hybrid system, the seasonal saving of electricity consumption (SSEC) is attained by integrating Eq. (13) over the entire summer cooling season (June-September) using the hourly weather data available in the form of CSWD:

$$SSEC = \frac{\int SEC dt}{\int dt} \approx \frac{\sum\limits_{cooling\ season} SEC\ \Delta t}{\sum\limits_{cooling\ season} \Delta t} \tag{14}$$

6 Results and discussions

6.1 Experiment and analysis results for all test conditions

The results for experiment and energy saving potential analysis for the test conditions with 11 ℃ WBD are shown in Table 3. For the test point 15, the inlet air dry-bulb temperature was 27 ℃, the REC provided full cooling load and the percentage saving of energy was 46.6%. With increasing the inlet dry-bulb and wet-bulb temperatures, supply air temperature produced by the REC was steadily growing and the percentage cooling provided by the REC was getting smaller. For the test point 20 with 37 ℃ inlet dry-bulb, the REC only offered 58.6% of total cooling load, also resulting in 46.6% of energy savings.

For all the test conditions, wet-bulb effectiveness of the REC experimental system as a function of intake air dry-bulb temperature for different WBDs is shown in Fig. 11.

The PREC values as a function of intake air DBT and WBD were calculated using experimental results of all test points, as shown in Fig. 12. It is found that the PREC has a decreasing trend with increasing DBT or reducing WBD of intake air. With the decreasing of WBD, the humidity of outdoor air is growing. In such humid conditions, performance of the REC will decline significantly, leading to lower PREC.

Fig. 13 depicts the percentage saving of electricity consumption (SEC) using REC and PUA hybrid system compared against stand-alone PUA unit. It can be seen that the highest SEC value was nearly 87%, as opposed to -22% of lowest value. The negative value was caused by the reduction in WBD value, which was only 3 ℃ for this condition. Our experiments indicated that REC's energy efficiency tends to decrease when it is exposed to more humid intake conditions, i.e. lower WBD. For this case, the power consumed by hybrid system outweigh that by stand-alone PUA, thus the energy would be wasted rather than saved.

6.2 Hourly energy-saving potential for summer design day

Fig. 14 shows profiles of hourly building cooling load and cooling capacity provided by the REC for the summer design day (21th.July) of Xi'an city. The figure also depicts power demands of the REC unit, hybrid REC and PUA system and the stand-alone PUA unit which was used to produce the same cooling with the hybrid system. The total difference between power demands of the hybrid system and the stand-alone PUA unit is the effective power savings achieved by the evaporative cooler. It is observed that a great deal of energy savings can be achieved between 13:00 and 19:00 h. Expect for this duration, we noticed that the cooling capacity provided by REC unit is higher than the cooling load from 1:00 to 13:00 h, thus for this period the REC has the capability of providing the whole cooling independently without participation of mechanical cooling system. However, between 13:00 and 20:00 h, the cooling capacity delivered by the REC is unable to cover the full cooling load. Under such situations, PUA has to be applied in combination with the REC unit, resulting in increased power demand. From 4:00 to 9:00 h, the cooling load has negative values due to lower outdoor

air temperature (less than indoor design temperature). In this case, to obtain maximum energy savings, we can use direct fresh air to provide cooling for the internal space and the REC unit should be suspended temperately without consuming power.

6.3 Analysis of hourly weather data and cooling hours

Monthly average outdoor air DBT and WBD for selected cities, as shown in Fig. 15 was evaluated from June to September using hourly dry-bulb and wet-bulb temperatures of CSWD. Guangzhou, Chongqing and Shanghai, representing the southern regions with hot and humid climates in summer, have the higher average DBT and smaller WBD compared to other locations. Urumqi, Lanzhou, Xi'an, representing the western regions with hot and dry climates, have both higher DBT and WBD. Comparatively, Harbin has the lowest average DBT and moderate WBD.

For each selected region, the total hours that require active cooling were summed up and indicated in Fig.16. It was obtained by adding up the total hours when hourly outdoor air DBT is higher than our specified indoor design temperature. The figure shows that Guangzhou has the longest cooling hours (68% of total summer hours), followed by Shanghai (53%) and Chongqing (53%). Urumqi (28%), Lanzhou (19%) and Harbin (15%) have the less cooling hours due to their distinct climatic conditions.

The hourly weather data of total cooling hours for each location were used to predict the follow-on monthly and seasonal values of PREC and SEC individually.

6.4 Monthly and seasonal energy-saving potential

The aforementioned analysis procedure used for estimating the hourly power demand and saving for Xi'an's summer design day was duplicated to calculate the hourly power savings for different cooling months and full cooling seasons of selected regions by utilising the cooling hours' hourly dry-bulb and wet-bulb temperature data.

The monthly and seasonal values of PREC for all selected regions were summarised in greater details in Table 4. For every month of summer season, REC can provide 44.2-100% of cooling load for all selected cities. It is concluded that, for the regions with hot and dry climate in summer, i.e. Urumqi, Lanzhou, Xi'an and Harbin, the REC can provide 90-100% of cooling load during whole cooling season. For the regions of Guangzhou, Shanghai and Chongqing with hot and humid climate, more than 50% of cooling demand can be supplied by the REC. Therefore, adopting the REC unit in mechanical cooling system is regarded as an effective approach to reduce the capacity of conventional air conditioning system.

Using hourly weather data of cooling hours, the monthly and seasonal percentage saving of electrical energy (SEC) were estimated and shown specifically in Table 5 and Fig. 17 respectively. It is found that the monthly SEC is ranged from 7.7% (Guangzhou) to 62.9% (Beijing), while the seasonal SEC varies from 13% (Shanghai, Guangzhou) to 58.7% (Urumqi). As expected, the highest seasonal SEC (over 50%) can be achieved for the locations of Urumqi, Lanzhou, Xi'an due to their high DBT and WBD. Comparatively, less seasonal SEC values were attained for Harbin (nearly 45%) and Beijing (nearly 41%), followed by Chongqing (28.4%).

13

7   Conclusions

The performance of a counter-flow REC prototype has been experimentally investigated under numerous typical outdoor air conditions of China. The experimental results obtained from the testing have been used to assess annual/seasonal reductions in cooling demands and energy consumptions of the REC system applied in China's various regions. The assessment method developed here is based on detailed calculations in terms of reductions in hourly cooling loads and hourly energy savings. This has been done by using the experimental outcomes and hourly climatic data of selected locations.

The major findings are concluded as bellows:

1)   Variation of cooling capacity provided by the REC and related energy savings as a function of outdoor air DBT (ranging from 27 to 37 ºC) for different WBD (3-17 ºC) have been found experimentally. This function relationship can be used to predict the energy-saving potentials of many other locations in the future.

2)   Average outdoor air DBT and WBD of all selected locations were presented by analysing hourly weather data of CSWD. Taking them into account, the suitability of evaporative cooling for different regions of China has been compared. The regions with high DBT and WBD are expected to have greatest energy-saving potential.

3)   By incorporating the REC into mechanical air conditioning system, nearly 53-100% of cooling load and 13-58% of power consumption could be reduced annually for several regions with varied typical climates. It confirms that the proposed REC is capable of creating significant energy savings when it is applied to cooling for different regions with various climates, even for hot and humid climate. Among these regions, the north-western regions, i.e. Urumqi, Lanzhou, and Xi'an city have the largest evaporative cooling and energy saving potentials, covering annual 93-100% cooling demands and bringing 53-59% energy saving reductions. The northern regions such as Beijing and Harbin have the moderate cooling capacity (84-96%) and energy saving potentials (41-45%). The south-eastern and south-western regions of China, including Shanghai, Guangzhou and Chongqing, have the least evaporative cooling availability (53-72%) and power consumption reductions (13-28%).

Apart from the remarkable benefit of energy savings, the REC can also provide 100% fresh air to improve indoor air quality of buildings. However, it is not always necessary to supply 100% fresh air to indoor spaces. Therefore, if the REC utilise part of interior return air as inlet air, more energy could be saved as a result. In this aspect, more field testing and evaluation work should be carried out in the future.

Acknowledgements

References

[1] M.-H. Kim, J.-W. Jeong, Cooling performance of a 100% outdoor air system integrated with indirect and direct evaporative coolers, Energy. 52 (2013) 245–257.

[2] P. Chen, H. Qin, Y.J. Huang, H. Wu, C. Blumstein, Energy-saving potential of precooling incoming outdoor air by indirect evaporative cooling, in: Proceedings of the 1993 Winter Meeting of ASHRAE Transactions, Chicago, United States, 1992.

[3] S. Delfani, J. Esmaeelian, H. Pasdarshahri, M. Karami, Energy saving potential of an indirect evaporative cooler as a pre-cooling unit for mechanical cooling systems in Iran, Energy Build. 42 (11) (2010) 2169–2176.

[4] X. Cui, K.J. Chua, M.R. Islam, K.C. Ng, Performance evaluation of an indirect pre-cooling evaporative heat exchanger operating in hot and humid climate, Energy Convers Manage. 102 (2015) 140-150.

[5] A. Youssef, A. Hamid, Energy saving potential of indirect evaporative cooling as fresh air pre-cooling in different climatic conditions in Saudi Arabia, in: 1st International Conference on Energy and Indoor Environment for Hot Climates, Doha, Qatar, 2014.

[6] W. Gao, W. Worek, V. Konduru, K. Adensin, Numerical study on performance of a desiccant cooling system with indirect evaporative cooler, Energy Build. 86 (2015) 16–24.

[7] M.-H. Kim, J.-Y. Park, M.-K. Sung, A.-S. Choi, J.-W. Jeong, Annual operating energy savings of liquid desiccant and evaporative-cooling-assisted 100% outdoor air system, Energy Build. 76 (2014) 538–550.

[8] M.-H. Kim, J.-S. Park, J.-W. Jeong, Energy saving potential of liquid desiccant in evaporative-cooling-assisted 100% outdoor air system, Energy. 59 (2013) 726–736.

[9] W.M. Worek, M. Khinkis, D. Kalensky, V. Maisotsenko, Integrated Desiccant–Indirect Evaporative Cooling System Utilizing the Maisotsenko Cycle, In: HT2012, Proc. of the ASME 2012 summer heat transfer conf., Rio Grande, Puerto Rico, USA, 2012.

[10] S.-W. Ham, S.-J. Lee, J.-W. Jeong, Operating energy savings in a liquid desiccant and dew point evaporative cooling-assisted 100% outdoor air system, Energy Build.116 (2016) 535–552.

[11] G.P. Maheshwari, F. Al-Ragom, R.K. Suri, Energy-saving potential of an indirect evaporative cooler, Appl Energy. 69 (2001) 69–76.

[12] A. Khandelwal, P. Talukdar, S. Jain, Energy savings in a building using regenerative evaporative cooling, Energy Build. 43 (2011) 581–591.

[13] X. Zhao, S. Yang, Z. Duan, S.B. Riffat, Feasibility study of a novel dew point air conditioning system for China building application, Building Environ. 44 (2009) 1990–1999.

[14] A. Hasan, Indirect evaporative cooling of air to a sub-wet bulb temperature, Appl Therm Eng. 30 (2010) 2460–2468.

[15] X. Zhao, Z. Duan, C. Zhan, S.B. Riffat, Dynamic performance of a novel dew point air conditioning for the UK buildings, Int J Low-Carbon Tech 4 (2009) 27–35.

[16] C. Zhan, Z. Duan, X. Zhao, S. Smith, H. Jin, S. Riffat, Comparative study of the performance of the M-cycle counter-flow and cross-flow heat exchangers for indirect evaporative cooling – Paving the path toward sustainable cooling of buildings, Energy. 36 (2011) 6790–6805.

[17] S. Anisimov, D. Pandelidis, A. Jedlikowski, V. Polushkin, Performance investigation of a M (Maisotsenko)-cycle cross-flow heat exchanger used for indirect evaporative cooling, Energy. 76 (2014) 593–606.

[18] Idalex. The Maisotsenko cycle-conceptual. A Technical Concept View of the Maisotsenko Cycle (2003). http://www.idalex.com/technology/how_it_works_-_engineering_perspective.htm.

[19] C. Zhan, X. Zhao, S. Smith, S.B. Riffat, Numerical study of a M-cycle cross-flow heat exchanger for indirect evaporative cooling, Building Environ. 46 (2011) 657–668.

[20] Z. Duan, C. Zhan, X. Zhang, M. Mustafa, X. Zhao, B. Alimohammadisagvand, A. Hasan, Indirect evaporative cooling: Past, present and future potentials, Renew Sustain Energy Rev. 16 (2012) 6823–6850.

[21] S. Anisimov, D. Pandelidis, Numerical study of the Maisotsenko cycle heat and mass exchanger, Int J Heat Mass Transf. 75 (2014) 75–96.

[22] S. Anisimov, D. Pandelidis, Theoretical study of the basic cycles for indirect evaporative air cooling, Int J Heat Mass Transf. 84 (2015) 974–989.

[23] D. Pandelidis, S. Anisimov, W.M. Worek, Comparison study of the counter-flow regenerative evaporative heat exchangers with numerical methods, Appl Therm Eng. 84 (2015) 211–224.

[24] M. Jradi, S. Riffat, Experimental and numerical investigation of a dew-point cooling system for thermal comfort in buildings, Appl Energy. 132 (2014) 524–535.

[25] P. Xu, X. Ma, T.M.O. Diallo, X. Zhao, K. Fancey, D. Li, H. Chen, Numerical investigation of the energy performance of a guideless irregular heat and mass exchanger with corrugated heat transfer surface for dew point cooling, Energy. 109 (2016) 803–817.

[26] Z. Duan, C. Zhan, X. Zhao, X. Dong, Experimental study of a counter-flow regenerative evaporative cooler, Building and Environ. 104 (2016) 47–58.

[27] O. Khalid, M. Ali, N.A. Sheikh, H.M. Ali, M. Shehryar, Experimental analysis of an improved Maisotsenko cycle design under low velocity conditions, Appl Therm Eng. 95 (2016) 288–295.

[28] D. Zube, L. Gillan, Evaluating Coolerado Corporation's heat-mass exchanger performance through experimental analysis, Int J Energy Clean Environ. 12 (2011) 101–116.

[29] B. Frank, On-site experimental testing of a novel dew point evaporative cooler, Energy Build. 43 (2011) 3475–3483.

[30] B. Riangvilaikul, S. Kumar, An experimental study of a novel dew point evaporative cooling system, Energy Build. 42 (2010) 637–644.

[31] J. Lee, D.-Y. Lee, Experimental study of a counter flow regenerative evaporative cooler with finned channels, Int J Heat Mass Transf. 65 (2013) 173–179.

[32] Coolerado Corporation, 4430 Glencoe St. Denver, CO 80216, USA. http://www.coolerado.com/.

[33] S.T. Hsu, Z. Lavan, W.M. Worek, Optimization of wet-surface heat exchangers, Energy. 14 (1989) 757–770.

[34] H.D.M. Hettiarachchi, M. Golubovic, W.M. Worek, The effect of longitudinal heat conduction in cross flow indirect evaporative air coolers, Appl Therm Eng. 27 (2007) 1841–1848.

[35] ASHRAE, ASHRAE Handbook: Fundamentals, American Society of Heating, Refrigerating and Air-Conditioning Engineers, Inc., Atlanta, 2009.

[36] China Meteorological Bureau-Climate Information Center-Climate Data Office and Tsinghua University-Department of Building Science and Technology, China Standard Weather Data for Analyzing Building Thermal Conditions, Beijing, China Building Industry Publishing House, 2005.

[37] L. Neal and D. O'Neal, The Impact of Residential Air Conditioner Charging and Sizing on Peak Electrical Demand, in: Proceedings of the 1992 Summer Study on Energy Efficiency in Buildings, American Council for an Energy Efficient Economy, Washington D.C., USA, 1992.

Table 1 Test samples of evaporative material

Index	Wicking material	Moisture-proof	Bonding treatment method
A	Kraft paper	none	none
B	Kraft paper	waxing	hot-melt
C	Kraft paper	aluminium foil	adhesive
D	cellulose-blended fibre	none	none
E	cellulose-blended fibre	aluminium sheet	hot melt polyethylene film
F	non-woven fabric	aluminium sheet	reactive hydrophilic adhesive
G	Kraft paper	aluminium sheet	hot melt polyethylene film
H	cellulose-blended fibre	aluminium sheet	reactive hydrophilic adhesive
I	Kraft paper	aluminium sheet	reactive hydrophilic adhesive

Table 2 0.4% cooling and evaporation design conditions for representative regions within China

Index	Region	Climate zone*	Std P kPa	Cooling			Evaporation		
				DBT °C	CWBT °C	RH %	WBT °C	CDBT °C	RH %
1	Urumqi	1	90.76	33.3	16.3	17.1	18	28.2	38.6
2	Xining	1	76.94	27.3	14.7	29.2	16.8	23.3	55.8
3	Lanzhou	2	84.37	32	17.7	26.5	20	27.8	51.4
4	Yinchuan	1	88.66	31.7	19.5	31.4	22.1	28.5	57.6
5	Beijing	2	100.67	35	22.2	33.1	26.9	30.6	75.3
6	Dalian	2	100.17	31.1	23.1	51.0	25.7	28.5	80.1
7	Lhasa	2	64.5	24.9	10.9	23.3	13.2	20.4	51.1
8	Kunming	3	80.57	27	16.7	38.6	20	24.3	69.7
9	Xi'an	2	96.63	35.6	23.3	36.3	26.2	31.9	64.6
10	Wuhan	4	101.05	35.4	27.4	54.6	28.4	33	71.1
11	Chongqing	4	97.18	36.4	25.8	43.3	27.2	32.7	65.7
12	Changsha	4	100.51	35.7	27	51.5	28	32.3	72.5
13	Shanghai	4	101.28	34.4	27.3	58.2	28	32.3	72.4
14	Guangzhou	5	101.23	34.8	26.5	52.5	27.7	31.5	75
15	Harbin	1	99.62	31.3	20.8	38.7	24.2	28.1	72.7

Table 3 Summary of experiment and energy saving analysis results for a few test conditions (WBD=11 ºC, V_3/V_1=0.5)

Test point	$t_{db,1}$ (ºC)	$t_{wb,1}$ (ºC)	$t_{db,2}$ (ºC)	ε_{wb} —	P_{REC} (kW)	Q_{REC} (kW)	Q_{in} (kW)	PREC (%)	SEC (%)
15	27	16	18.8	0.747	0.068	0.305	0.126	100	46.6
16	29	18	20.5	0.772	0.068	0.310	0.208	100	68.1
17	31	20	22.4	0.786	0.068	0.311	0.289	100	77.8
18	33	22	24.2	0.799	0.068	0.310	0.368	84.2	64.9
19	35	24	26.1	0.810	0.068	0.309	0.447	69.1	54.2
20	37	26	28.0	0.820	0.068	0.307	0.524	58.6	46.6

Table 4 Monthly and seasonal percentage of cooling provided by REC unit

City	June	July	August	September	Cooling season
	%	%	%	%	%
Urumqi	100.0	100	100	100	100
Lanzhou	100	100	100	100	100
Beijing	99.5	72.9	79.2	96.9	84.3
Xi'an	99.2	86.5	93.8	99.2	92.9
Chongqing	73.9	65.7	71.4	90.7	72.5
Shanghai	59.5	58.9	57	88.1	62.0
Guangzhou	55.1	44.2	49.3	69.6	53.3
Harbin	99.5	97.5	89.8	100	95.9

Table 5 Monthly percentage saving of electricity consumption for selected cities

City	June	July	August	September
-	%	%	%	%
Urumqi	54.5	60.5	59.7	59.8
Lanzhou	56.5	61.3	49.7	48.8
Beijing	62.9	27.2	35.2	45.9
Xi'an	59.9	46.3	54.1	54.8
Chongqing	22.4	24.4	30.8	42.4
Shanghai	11.9	13.3	8.5	23.8
Guangzhou	13.2	10.6	7.7	26.4
Harbin	52.2	46.9	33.7	43.2

(a)

(b)

Fig. 1. Graphs showing working principle and psychrometric process of (a) M-cycle multi-stage regenerative HMX [18] (b) single-stage regenerative HMX.
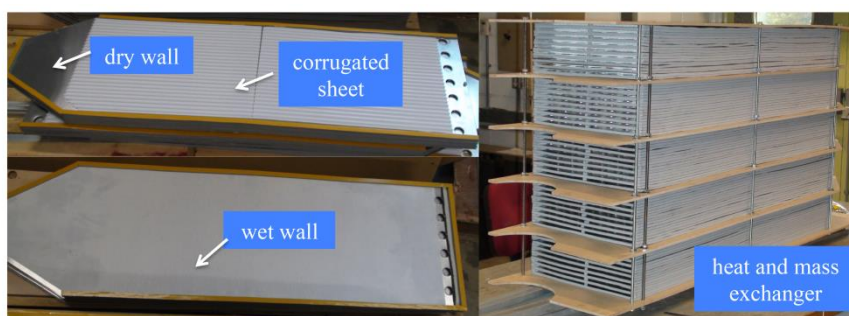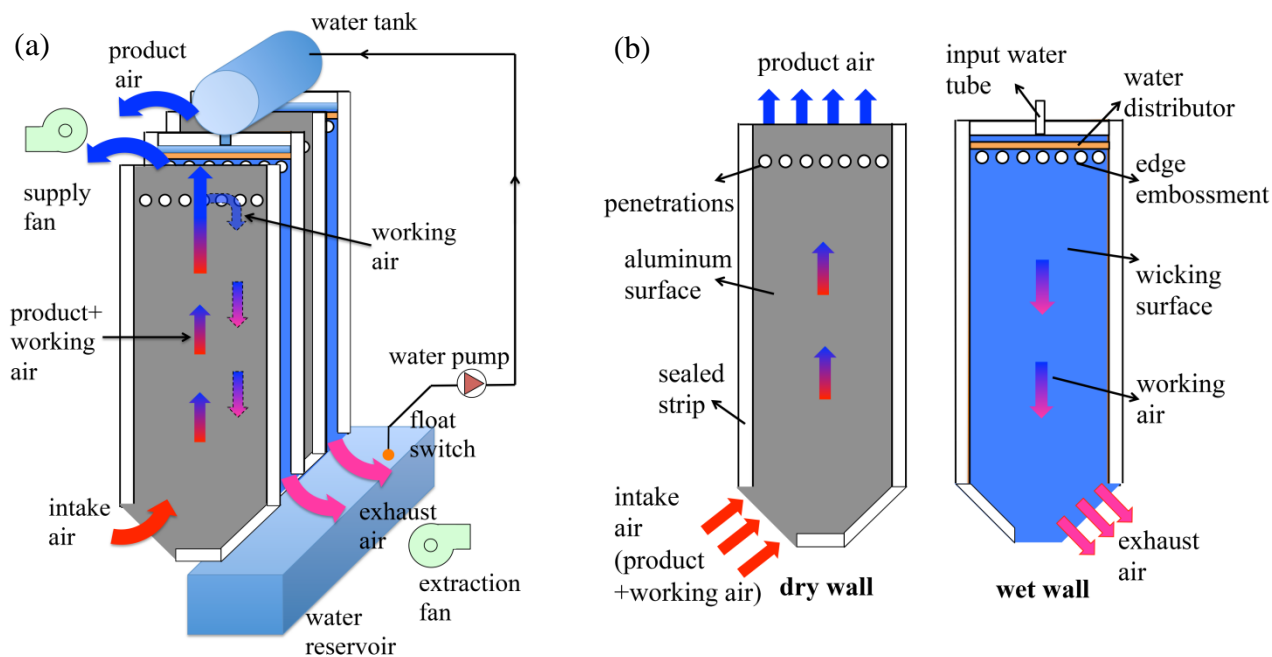
Fig. 2. Graphs showing schematics of (a) the developed counter-flow REC system, (b) the heat exchanging walls with corrugated air guiders and (c) images of the heat exchanging walls and HMX fabricated in laboratory.
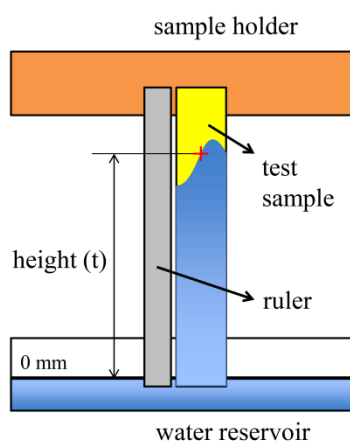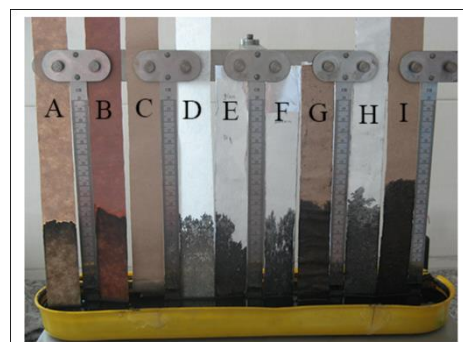
Fig. 3. Graphs showing the (a) schematic of test apparatus of vertical wicking height and (b) image of experimental set-up.
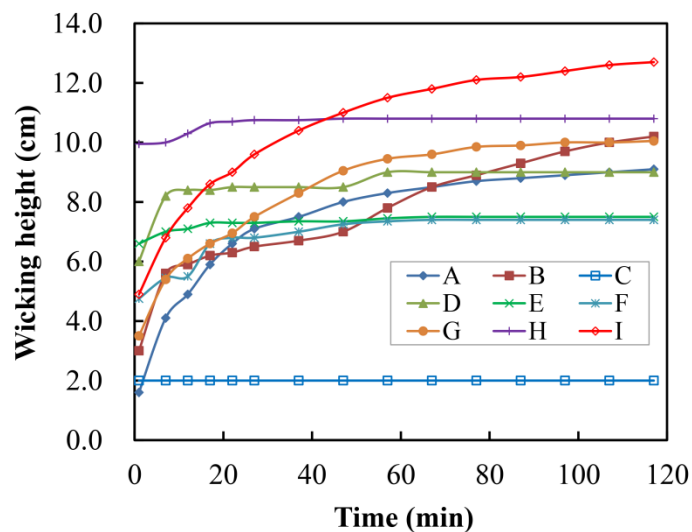
Fig. 4. Wicking height as a function of time.
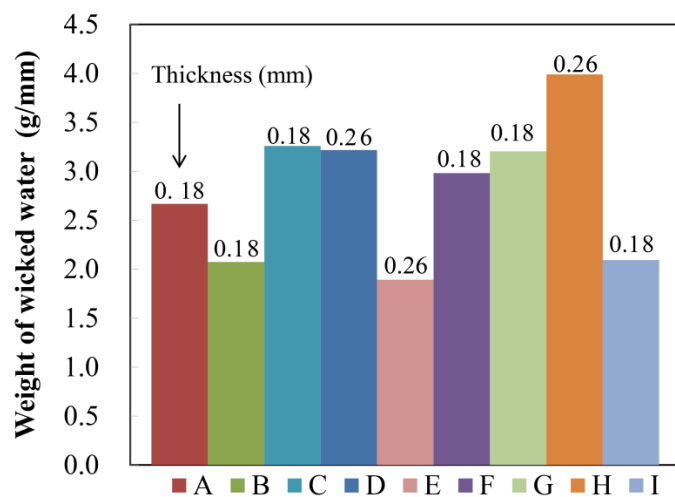
Fig. 5. Wicked weight of water per unit thickness for test materials.
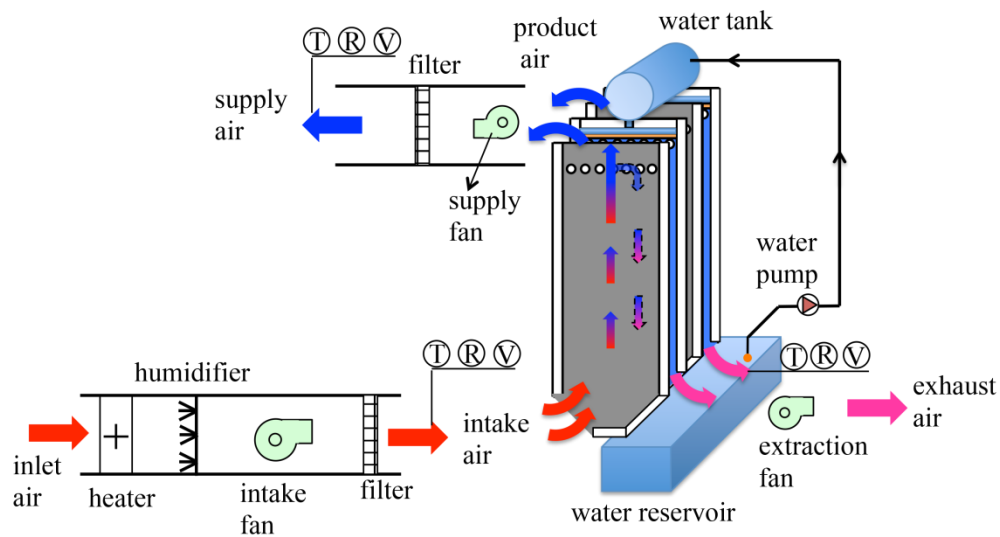
Fig. 6. Schematic of experimental set-up.
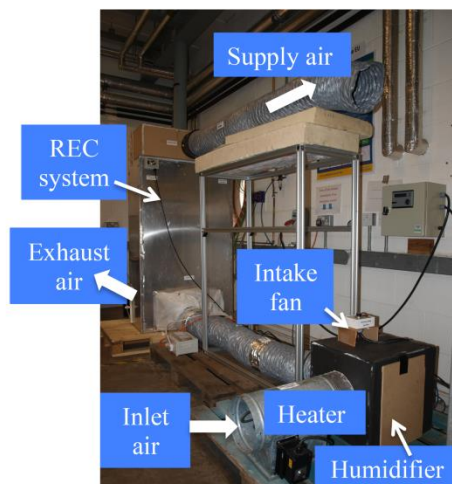
Fig. 7. View of the experimental set-up.
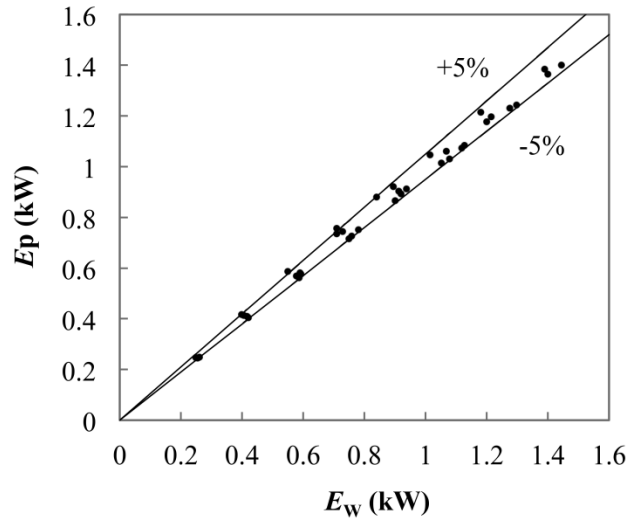
Fig. 8. Comparison between energy changes in product and working air.
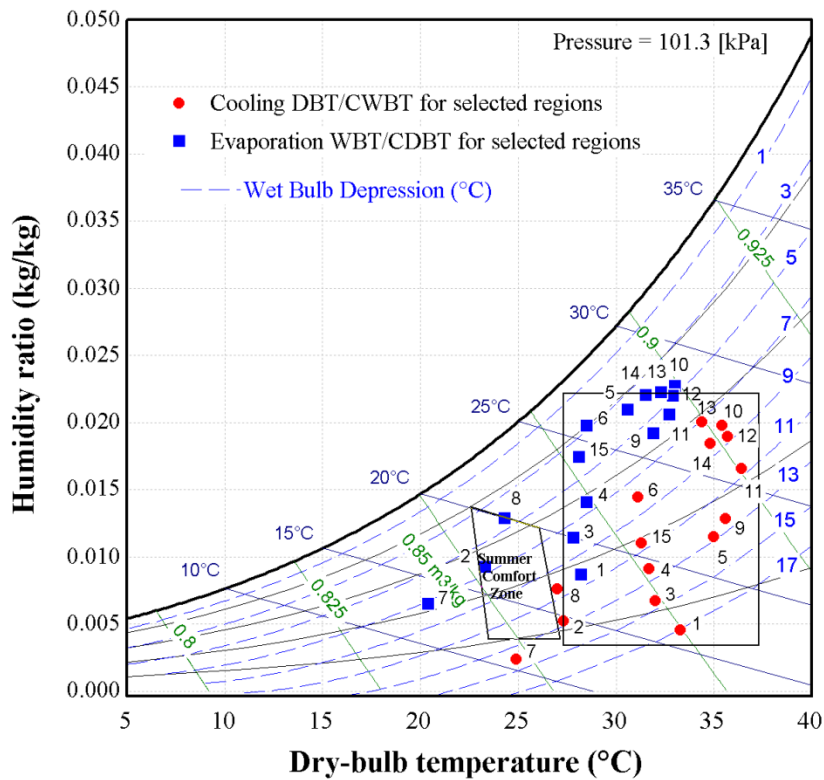
Fig. 9. Psychometric chart showing 0.4% cooling and evaporation design conditions for representative regions within China.
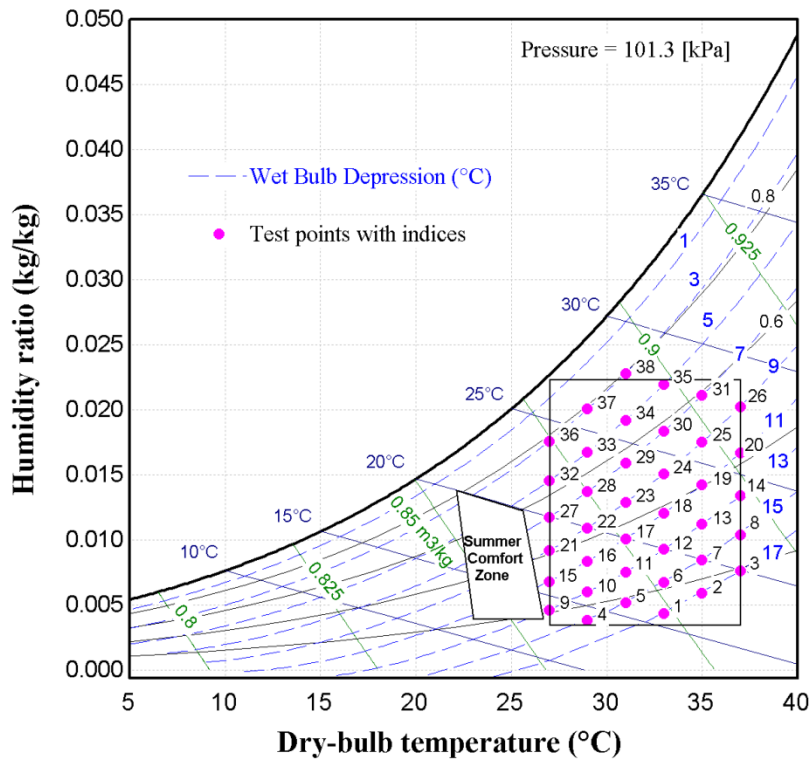
Fig. 10. Psychometric chart showing all test points.
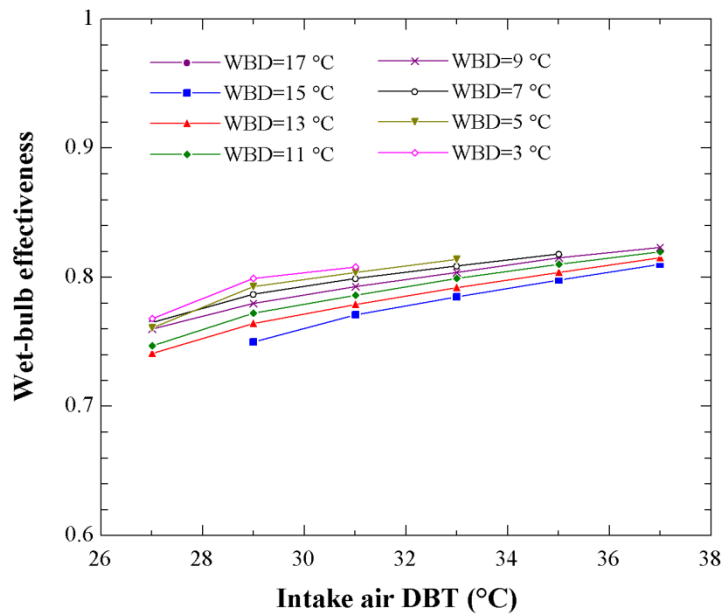
Fig. 11. Wet-bulb effectiveness of the REC experimental system as a function of intake air dry-bulb temperature for different WBDs (all test conditions).
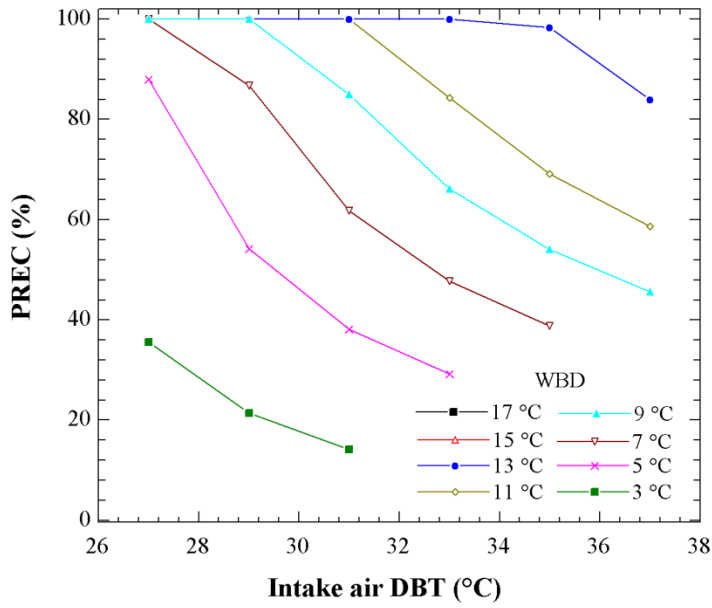
Fig. 12. Percentage cooling provided by the REC in hybrid system (all test conditions).
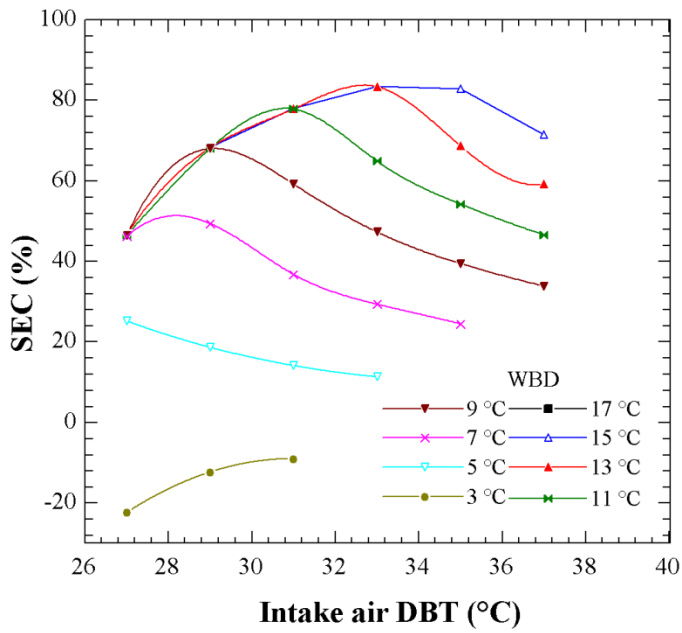
Fig. 13. Percentage saving of electricity consumption for all test conditions.
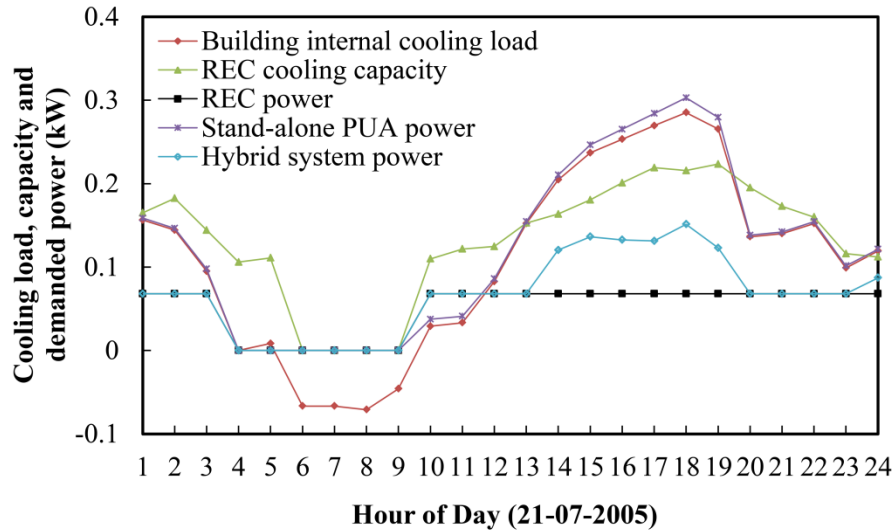
Fig. 14. Hourly profiles of building cooling load, cooling capacity of REC and power demands of REC, stand-alone PUA and hybrid system for Xi'an.
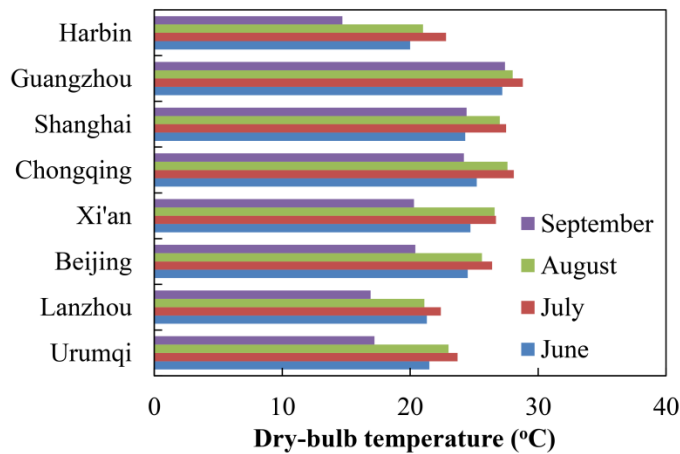
(a)
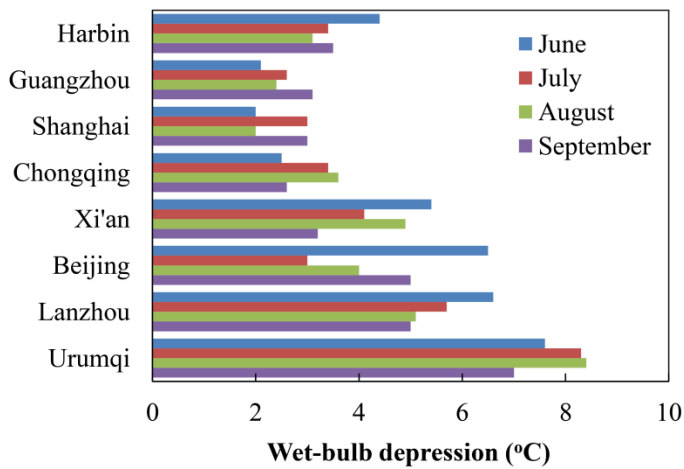
(b)

Fig. 15. Monthly average (a) outdoor air dry-bulb temperature and (b) wet-bulb depression for selected cities during cooling season.
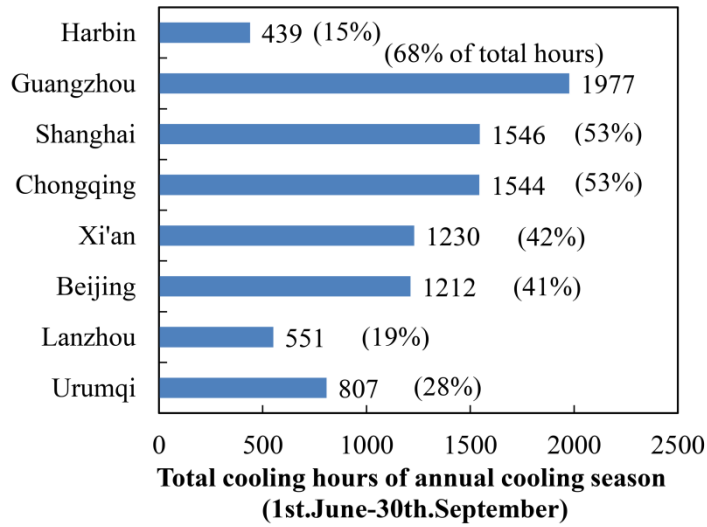
Fig. 16. Total cooling hours of annual cooling season for selected cities.

Fig. 17. Seasonal saving of electricity consumption for selected cities.